MERGER RATES OF DOUBLE NEUTRON STARS AND STELLAR ORIGIN BLACK HOLES: THE IMPACT OF INITIAL CONDITIONS ON BINARY EVOLUTION PREDICTIONS

S. E. de Mink[1] and K. Belczynski[2,3]

[1] Anton Pannenkoek Astronomical Institute, University of Amsterdam, 1090 GE Amsterdam, The Netherlands (S.E.deMink@uva.nl)
[2] Astronomical Observatory, Warsaw University, Al. Ujazdowskie 4, 00-478 Warsaw, Poland (kbelczyn@astrouw.edu.pl)
[3] Warsaw Virgo Group

Draft version July 16, 2018

ABSTRACT

The initial mass function (IMF), binary fraction and distributions of binary parameters (mass ratios, separations and eccentricities) are indispensable input for simulations of stellar populations. It is often claimed that these are poorly constrained significantly affecting evolutionary predictions. Recently, dedicated observing campaigns provided new constraints on the initial conditions for massive stars. Findings include a larger close binary fraction and a stronger preference for very tight systems. We investigate the impact on the predicted merger rates of neutron stars and black holes. Despite the changes with previous assumptions, we only find an increase of less than a factor 2 (insignificant compared with evolutionary uncertainties of typically a factor $10 - 100$). We further show that the uncertainties in the new initial binary properties do not significantly affect (within a factor of 2) our predictions of double compact object merger rates. An exception is the uncertainty in IMF (variations by a factor of 6 up and down). No significant changes in the distributions of final component masses, mass ratios, chirp masses and delay times are found. We conclude that the predictions are, for practical purposes, robust against uncertainties in the initial conditions concerning binary parameters with exception of the IMF. This eliminates an important layer of the many uncertain assumptions affecting the predictions of merger detection rates with the gravitational wave detectors aLIGO/aVirgo.

Subject headings: stars: black holes, neutron stars, x-ray binaries

1. INTRODUCTION

These are very exciting times for gravitational wave astrophysics. The direct detection of the gravitational wave signal of the merger of two compact objects, neutron stars (NS) or black holes (BH) is anticipated before the end of this decade.

Gravitational waves are a natural consequence of the theory of General Relativity (Einstein 1918). They are perturbations of the spacetime metric propagating at the speed of light, which are generated, for example, during the inspiral of two compact objects. Indirect evidence for the existence of gravitational waves was provided by the orbital decay of the Hulse-Taylor pulsar (Hulse & Taylor 1975; Taylor & Weisberg 1989) and later with stronger constraints by the double pulsar (Burgay et al. 2003; Lyne et al. 2004). Direct detection of the gravitational wave signal of the inspiral of NS-NS, BH-NS or BH-BH binaries and the subsequent merger and ring down is expected to happen in the next few years, now the advanced ground-based gravitational wave detectors aLIGO and Virgo are coming online (Abbott et al. 2009; Caron et al. 1997).

The initial LIGO/Virgo observations were concluded in 2010 without detection, but they provided upper limits on the merger rates (Abadie et al. 2012). The advanced version of the detectors will be approximately 10 times more sensitive than the initial versions, expanding the detection volume and thus the chance of detection by a factor of about a thousand (Aasi et al. 2013c).

The first science run of advanced LIGO is scheduled for late 2015 (Aasi et al. 2013b). A detection during the first science run is not considered to be likely, but one or more detections are anticipated in the next few years as the sensitivity increases to a range of 200 Mpc for double neutron stars. This translates to $\sim$ 0.2–200 expected detections double neutron star mergers per year (Aasi et al. 2013b). Even without detections, the new upper limits will become astrophysical interesting as they start to rule out the models that predict the highest merger rates (Mandel & O'Shaughnessy 2010; Belczynski et al. 2012a; Stevenson et al. 2015).

Obtaining reliable predictions of the merger rates of relativistic compact objects has been a very large challenge, as reviewed by (Abadie et al. 2010). The rates quoted above are derived semi-empirically using the observed binary pulsars in our Galaxy (Phinney 1991; Kalogera et al. 2004). The large uncertainties result from the small size of the sample of observed binary pulsars and the pulsar luminosity distribution. The implicit assumption is made that the observed sample is representative for the Galactic population. Further constraints come from short gamma-ray bursts, but the rate estimates depend on the uncertain luminosity function and opening angle of the jets (e.g. Fong et al. 2012). Type Ibc supernovae have served so far as ultimate upper limits (Kim et al. 2010). The merger rates for BH-NS and BH-BH systems are even more problematic as we lack direct observational evidence of their existence. However, some immediate progenitors for BH-BH (e.g. Bulik et al. 2011) and BH-NS systems (e.g. Grudzinska et al. 2015) have been proposed.

Even though theoretical predictions suffer from even larger uncertainties, they have been crucial to estimate

the merger rates involving black holes. They further provide the expected distribution of properties for all merger types including for example the delay times, component and chirp masses. More importantly, the theoretical predictions are providing the tool for future comparison with the detections, crucial to identify what gravitational wave signals teach us about the astrophysics of the progenitor systems (e.g. Stevenson et al. 2015). Several groups have presented similar estimates and studies in the past decade (e.g. Lipunov et al. 1997; Bethe & Brown 1998; De Donder & Vanbeveren 1998; Bloom et al. 1999; Grishchuk et al. 2001; Nelemans et al. 2001; Voss & Tauris 2003; Dewi & Pols 2003; Nutzman et al. 2004; De Donder & Vanbeveren 2004; Pfahl et al. 2005; Postnov & Yungelson 2006; Yungelson et al. 2006; O'Shaughnessy et al. 2008, 2010; Dominik et al. 2012, 2013; Mennekens & Vanbeveren 2014; Dominik et al. 2015).

For all predictions we can distinguish several sources of uncertainty: (I) the adopted *initial conditions* in the simulations, (II) the uncertainties in the *physics of the stellar evolution and binary interaction*, (III) the uncertainties associated with the *normalization* of the merger rates, which include the mapping to the appropriate star formation history of the detection volumes and (IV) modeling of the *detectability* of gravitational waves from the predicted merger events.

Recent observations have provided new constraints on the initial conditions and primordial binary properties (Kobulnicky & Fryer 2007; Kiminki & Kobulnicky 2012; Chini et al. 2012; Sana et al. 2012; Sana et al. 2013, 2014; Kobulnicky et al. 2014; Moe & Di Stefano 2015a,b; Dunstall et al. 2015), for a review see (Duchêne & Kraus 2013). The studies show that the initial conditions for young massive stars differ substantially from the initial conditions that have typically been adopted to simulate compact object mergers coming from binary evolutionary channels.

Among the most striking findings are (i) the large fraction massive stars that have a companion close enough to interact by exchanging mass before they die and (ii) the preference for very tight binaries with orbital periods of a few days, implying that a large fraction of massive stars will interact even before leaving the main sequence. Further findings include (iii) the confirmation of a flat distribution of mass ratios, ruling out a distribution that is strongly peaked to equal masses and (iv) a distribution of eccentricities that favors circular systems in stark contrast with the typically adopted thermal eccentricity distribution which favors eccentric systems.

The first two conclusions depend on adopted model of stellar evolution and in particular they require at least modest radial expansion for the majority of massive stars. The amount by which stars expand is considerably uncertain for high mass stars. Note that some very rapidly rotating massive stars may actually decrease in size as they evolve (Yoon & Langer 2005), possibly even preventing interaction with companion by mass transfer (de Mink et al. 2009) in very tight systems. For example, let us consider the fraction of massive binary systems in which mass transfer starts already during the main sequence evolution of the primary star. This depends on the maximum radius that a star reaches on the main sequence which depends on a number of rather uncertain processes such as convection and overshooting, (e.g. cali-

brations by Pols et al. 1997; Ribas et al. 2000; Brott et al. 2011a), further mixing processes such as those induced by rotation (e.g. Yoon & Langer 2005; Brott et al. 2011b; Ekström et al. 2012; Szécsi et al. 2015), mass loss by stellar winds and eruptions (review by Smith 2014) and the possible density inversions in the outer layers of massive stars which can result in inflated envelopes(e.g. Yusof et al. 2013; Köhler et al. 2015, and Jiang et al. 2015, subm.). Varying the maximum radius of main sequence stars by 30% up and down and allowing for uncertainties in the initial distributions, we find a large variation for this fraction, $20\% - 50\%$[1].

A further caveat to keep in mind is that the observations are limited to regions nearby such as our own Galaxy and the Magellanic Clouds which only cover metallicities down to about one fifth of the solar value. Also the regime of the highest mass stars is not well probed. Sana et al. (2012) observations cover stars in mass range $15 - 60 M_\odot$, but most of these are towards the lower end of this mass range. For low metallicities and higher star masses we have no direct constraints and the uncertainties in the evolutionary models start to play a larger role. Despite several attempts, no trends with metallicity or environment are found so far (e.g. Bastian et al. 2010; Moe & Di Stefano 2013). We extend Sana et al. (2012) distributions in our study to the entire range that can produce double compact objects ($M_{\rm zams} = 5 - 150 M_\odot$) and to a broad range of metallicities ($Z = 0.002 - 0.02$) as discussed in Section 2.

In this study we focus on the binary formation channels (in contrast to the dynamical formation channels that may occur in dense star clusters, e.g. Ivanova et al. 2008; Banerjee et al. 2010; Aarseth 2012; Clausen et al. 2013; Samsing et al. 2014; Ramirez-Ruiz et al. 2015). We investigate two questions: (i) What are the implications of the new initial conditions? and (ii) How robust are the predictions against the allowed variations in the new initial conditions resulting from the observational uncertainties.

For this purpose we perform a comparative population synthesis study where we use the recent work by Dominik et al. (2012) as a reference. We simulate the evolution of massive binary systems following the evolutionary channels for the formation of double compact objects. In Sect. 2 we describe the new and old initial conditions. In Sect. 3 we give a brief description of our computational method, the physical assumptions and computation of the merger rates. In Sect. 4 we compare the old and new initial distributions for the entire simulated populations and for the progenitors of double compact object mergers. In Sect. 5 we discuss the impact on the resulting merger rates. Finally, in Sect. 6 we present our discussion and conclusions.

2. INITIAL DISTRIBUTIONS

2.1. *New standard model (N) and its variations*

Recent dedicated observing campaigns have provided new constraints on the binary properties of young mas-

---

[1] This estimate was done with the `StarTrack` population synthesis code described in Section 3 considering systems with primary masses in the range $15 - 150 M_\odot$. The initial distributions of period and eccentricity were altered within limits listed in Section 2.1 assuming a binary fraction of 100%.

sive stars. Here, we investigate the impact of the distributions obtained by the work of Sana et al. (2012). This study is based on an intense spectroscopic monitoring spanning a decade surveying all O-type stars in six nearby ($\lesssim 3\,\mathrm{kpc}$) very young (about $2\,\mathrm{Myr}$ old) open star clusters and associations. Even though the sample may seem of modest size it exceeds previous studies in completeness in terms of the fraction of systems for which orbital solutions have been obtained. It provided an average of 20 radial velocity measurements for all 71 systems in the open clusters/associations that contain at least one O-star. This dataset includes orbital solutions for several long period systems (between 100 and 1000 days) which are very challenging as they require a long term observing campaign. This sample allowed a robust derivation of the underlying distribution of binary parameters after correction for incompleteness and biases.

The very young ages, relatively low densities and velocity dispersion of the stars, imply that the effects of stellar evolution and dynamical interactions are minimal. This makes this sample the most suitable to provide constraints on the primordial binary properties and thus the initial conditions for our simulations.

The primary stars in this sample have spectral types ranging from O9.7 to O3, which correspond approximately to a mass range from 15 to 60 $M_\odot$. This is appropriate for the progenitor systems of double compact object mergers that involve at least one black hole. Lower mass binaries may dominate the formation of double neutron stars.

The most suitable study for this mass range is provided by Dunstall et al. (2015) for the early B-type stars in the 30 Dor region and the Cygnus OB2 sample analyzed by Kobulnicky et al. (2014), which contains stars down to spectral types of B2.5V, which approximately corresponds to 8 $M_\odot$. Wright et al. (2015) infer an age spread for this region of 1-7 Myr. Statistically the findings by Kobulnicky et al. (2014) and Dunstall et al. (2015) are consistent with the distributions by Sana et al. (2012), although the results by Kobulnicky et al. (2014) and Dunstall et al. (2015) favor a flatter period distribution and a lower close binary fraction, similar to the old initial distributions that we use as reference (see Sec. 2.2). Whether this is a sign of a trend with decreasing primary mass, or whether the distribution of ages play a role is not clear.

Sourcing from our conclusions, we find that the changes in the period distribution have a rather small impact on double compact merger rates. Thus we apply the Sana et al. (2012) distributions as our new initial conditions for both O and early B stars for consistency.

Orbital periods— For the distribution of orbital periods, p, we adopt the distribution Sana et al. (2012) which significantly favors short period systems. Such a preference had been observed in previous surveys uncorrected for biases (e.g. Mason et al. 2009), but was generally interpreted as being the result of selection effects. Sana et al. (2012) demonstrated that this preference remains even after carefully correcting for observational biases. We adopt

$$f_p(\log p) \propto (\log p)^\pi, \qquad \text{for } \log p \in [0.15, 5.5] \qquad (1)$$

where p is given in days. For our standard simulation we adopt $\pi = -0.5$. We change the slope of orbital period distribution from $\pi = -0.75$ in model N-p1 to $\pi = -0.35$ in model N-p2.

Note that the spectroscopic observations can only reliable probe systems with $\log p \lesssim 3.5$. However, wider systems can still produce double compact object mergers as we will show in the following section. For wider systems we adopt the simplest assumption we can take and extrapolate the distribution, since we have no reasons to believe that the binary fraction suddenly drops beyond $\log p = 3.5$.

This assumption is consistent with the recent findings by interferometric studies of nearby Galactic massive stars. Sana et al. (2014) provided a large systematic survey probing companions of O stars at angular separations between 1 and 100 mili-arcseconds. For unevolved massive stars (O stars with luminosity class V) the detected companion fraction reaches 100% at 30 mili-arcseconds. The physical separations this corresponds to will remain uncertain until more accurate distance measurements become available. Roughly it corresponds to physical separations of 60-6000 AU. In our preferred units for the orbital separation a this corresponds to $\log a(\,R_\odot) = 4.1$-6.1. Considering systems with typical masses we find that our extrapolation of the orbital period distribution and binary fraction are consistent with these observations.

Mass ratios— For the distribution of mass ratios, which we define as the mass of the initially less massive star over the mass of the more massive star, i.e. $q \equiv M_2/M_1$, we use

$$f_q(q) \propto q^\kappa, \qquad \text{for } q \in [0.1, 1] \qquad (2)$$

where $\kappa = -0.1 \pm 0.6$ according Sana et al. (2012). We adopt $\kappa = 0$ such that the distribution becomes uniform distribution, which has also been found in several recent studies such as Kobulnicky & Fryer (2007) and Kobulnicky et al. (2014). To consider the uncertainties we consider lower and upper limits of $\kappa = 0.5$ in model N-q1 to $\kappa = -0.7$ in model N-q2.

We note that the most recent observations rule out the presence of a so-called twin population of equal mass systems (Pinsonneault & Stanek 2006). The idea of the possible existence of such a population gained interest as it favors the formation of double compact object mergers, in particular through the so-called double core formation channel proposed by Dewi et al. (2006). However, the claimed evidence of such a population has been demonstrated to be the result of observational biases towards equal mass systems that were not accounted for (Lucy 2006; Sana et al. 2013; Cantrell & Dougan 2014).

Eccentricities— For the eccentricity distribution in the very young open clusters Sana et al. (2012) finds

$$f_e(e) \propto e^\eta, \qquad \text{for } e \in [0.0, 0.9] \qquad (3)$$

with $\eta = -0.42 \pm 0.17$. The very short period systems ($p \lesssim 4$ days) show a larger degree of circularization as expected from the short time scale for tidal circularization (Zahn 1975). Unfortunately the data sample is not large enough to provide a reliable separation dependent eccentricity distribution. Instead we adopt this distribution as initial distribution for our simulations, independently

of the period. We explicitly follow the effects of tides in our simulations, which quickly circularizes the shortest period systems, consistent with the observations. As we will show later this assumption is justifiable as the variations in the eccentricity result in only minimal changes in the rates. In our standard simulation N we adopt $\eta = -0.42$. We consider uncertainties by changing the the slope to $\eta = -0.59$ in model N-e1 to $\eta = -0.25$ in model N-e2.

Binary fraction— The spectroscopic survey by Sana et al. (2012) yields a binary fraction of $f_{SB} = 0.7 \pm 0.1$ after correcting for biases. The binary fraction here is defined as

$$f_{bin} \equiv \frac{N_{bin}}{N_{bin} + N_{single}} \qquad (4)$$

where N_{bin} and N_{single} are the number of binary systems and the number of single stars respectively.

This fraction refers only to systems that have orbital parameters within the considered boundaries , i.e. $q \in [0.1, 1]$, $\log p(\text{days}) \in [0.15, 3.5]$ and $e \in [0.0, 0.9]$. The remainder of the sample ($\sim 30\%$) consists of stars of unknown nature, including wider binaries, binaries with more extreme mass ratios and possibly genuine single stars. Motivated by the interferometric survey (Sana et al. 2014) we designate the remainder as wide binaries. We extrapolate the original Sana et al. (2012) period distribution that extends to $\log p = 3.5$ to $\log p = 5.5$. Such extrapolation results in a binary fraction, including wide systems, of $f_{bin} = 1$. We also consider a reduced binary fraction of $f_{bin} = 0.85$ in model N-f1 and $f_{bin} = 0.7$ in model N-f2.

Masses— The observed distribution of primary masses in the sample of Sana et al. (2012) is consistent with a standard Kroupa (2002) mass function. Although we only simulate the evolution of massive binaries, for normalization we adopt the three component power law for the primary mass or single star m_1, given in solar units $M_\odot$

$$f_{m_1}(m_1) \propto \begin{cases} m_1^{-1.3}, & \text{for } m_1 \in [0.08, 0.5] \\ m_1^{-2.2}, & \text{for } m_1 \in [0.5, 1.0] \\ m_1^{-\alpha}, & \text{for } m_1 \in [1, 150] \end{cases} \qquad (5)$$

We adopt $\alpha = 2.7$ in our standard model, consistent with the field star population (Kroupa et al. 1993; Kroupa & Weidner 2003). To allow for uncertainties we consider $\alpha = 3.2$ in model N-m1 and $\alpha = 2.2$ in model N-m2.

2.2. *Old standard model (O) and its variations*

We adopt the Dominik et al. (2012) reference model as the old standard model O. In their work systems are drawn from an initial distribution of separations instead of orbital periods. This distribution is assumed to be flat in the log (Abt 1983; Öpik 1924)

$$f_a(\log a) \propto \text{constant}, \qquad \text{for } \log a \in [a_{min}, 5]. \qquad (6)$$

The lower boundary a_{min} is assumed to be a function of the stellar radii of the primary and secondary star at the zero age main-sequence (ZAMS),

$$a_{min} \equiv \frac{2R_{ZAMS,1} + 2R_{ZAMS,2}}{1 - e} \qquad (7)$$

This was adopted to ensure that at zero age both stars are well within their Roche lobes at closest approach, i.e. the periastron distance $d_{per} = a(1 - e)$. The distribution of mass ratios is a pseudo-flat distribution. The only difference with the new distribution concerns the boundaries. Dominik et al. (2012) consider $q \in [q_{min}, 1]$ with $q_{min} = 0.08/m_1$ to avoid selecting secondaries below H-burning limit. For the distribution of eccentricities a thermal-equilibrium distribution is adopted (Heggie 1975), which favors eccentric systems:

$$f_e(e) \propto e, \qquad \text{for } e \in [0, 1]. \qquad (8)$$

The binary fraction adopted by Dominik et al. (2012) is $f_{bin} = 0.5$, corresponding to the parameter boundaries specified above. For comparison we also provide estimates based on the old distribution but assuming a high binary fraction of $f_{bin} = 1$ in model O-f1.

The distribution of primaries masses (and single star masses) is identical to the one we adopt in the new reference model, given in Eq 5.

3. COMPUTATIONAL METHOD

For the purpose of this study we use the binary population synthesis code `StarTrack` (Belczynski et al. 2002, 2008), which has been used extensively to simulate the evolutionary channels and formation rates of compact objects www.syntheticuniverse.org. The suite of our simulations is available on this website.

This code belongs to a family of very fast and stable binary evolutionary codes, that provide powerful tools to explore the vast multi-dimensional space of the initial parameters that determine the fate of a binary system. These codes also enable the exploration of the effect of model uncertainties. These codes relay on precomputed grids of detailed stellar models and approximate treatments of the physical processes as described below. Despite the approximations, studies with this and similar codes based on the same philosophy have enabled insights into the many exotic phenomena resulting from low and high mass interacting binaries (e.g. recent work by Izzard et al. 2004, 2006, 2009; Ruiter et al. 2009; Mennekens et al. 2010; Vanbeveren et al. 2013; Fragos et al. 2013; Abate et al. 2013; de Mink et al. 2013, 2014; Toonen et al. 2014; Kochanek et al. 2014; Claeys et al. 2014; Mennekens & Vanbeveren 2014; Ruiter et al. 2014; Schneider et al. 2014, 2015)

A full description of the `StarTrack` code used in this study and assumptions concerning the treatment of stellar evolution and binary interaction can be found in the papers above Belczynski et al. (2002, 2008), Dominik et al. (2012) and references therein. Below we provide a summary of the main assumptions relevant for this study.

3.1. *Physical assumptions*

This study is a comparative study of the impact of the initial conditions. Dominik et al. (2012) is used as our reference model. We use Dominik et al. (2012), also when the assumptions are uncertain.

Stellar evolution— The code is based on detailed, but non rotating, single stellar evolutionary models by Pols et al. (1998). For this purpose the code utilizes the fit formula to the detailed models by Hurley et al. (2000) with several adaptations described in Belczynski et al.

(2002). The effects of mass loss and accretion are simulated using algorithms originally developed by (Tout et al. 1997; Hurley et al. 2002) to account for effects such as rejuvenation of the accreting star when appropriate.

Stellar wind mass loss— We employ updated wind mass loss rates, which include winds mass loss from early-type stars (Vink et al. 2001), Wolf-Rayet stars (Hamann & Koesterke 1998; Vink & de Koter 2005) and enhanced mass loss rates for Luminous Blue Variables calibrated to account for the observed distribution of masses of known black holes (Belczynski et al. 2010; Orosz et al. 2011). As a result the simulations allow for the formation of black holes with masses up to $15\,M_\odot$ in a solar metallicity environment. For sub-solar metallicity environments ($Z = 0.006$), black holes up to $30\,M_\odot$ are produced, consistent with the mass of the most massive known stellar-origin black hole in the IC10 X-1 system (Prestwich et al. 2007; Silverman & Filippenko 2008). Under these assumptions the simulations predict the formation of black holes with masses up to $80\,M_\odot$ in low metallicity ($Z = 0.0002$) environments for stars below initial mass of $150\mathrm{M}_\odot$.

Roche-lobe overflow and common envelope evolution— To determine whether mass transfer through Roche-lobe overflow is stable we consider the stellar type of the donor and mass ratio as outlined in (Belczynski et al. 2008). In the case of stable mass transfer, we assume that half of the mass lost by the donor is accreted by the companion. The remainder is leaving the system carrying a specific angular momentum of $2\pi a^2/P$, where a and P are the orbital separation and period following Podsiadlowski et al. (1992). Common envelope evolution is accounted for using the classical energy balance formalism (Webbink 1984) adopting a value of $\alpha_{\mathrm{CE}} = 1$ for the envelope efficiency parameter. The parameter λ describing the binding energy of the envelope is taken from fits by Xu & Li (2010a,b), implemented as described in Dominik et al. (2012).

Remnant masses for compact objects— To obtain the final mass of the compact objects, we consider the formation of a proto-neutron star and subsequent fall back of material. These are inferred to be a function of the carbon oxygen core mass as outlined in Section 4.2 of Fryer et al. (2012). The employed scheme utilizes the rapid supernova model that is able to reproduce the apparent mass gap between NSs and BHs (Belczynski et al. 2012b). We also account for the formation of neutron stars by electron capture supernovae (e.g. Nomoto 1984; Podsiadlowski et al. 2004) as outlined in Section 4.4 of Fryer et al. (2012). For single stars this effectively results in the formation of neutron stars for initial stellar masses above $7.6\,M_\odot$. The transition from neutron star to black hole is set at a mass of $2.5\,M_\odot$ for the resulting compact object. For high metallicity ($Z = 0.02$) this makes single stars above initial mass of $21\mathrm{M}_\odot$ to form BHs.

Supernova kicks— We account for the classical Boersma-Blaauw kick (Boersma 1961; Blaauw 1961) resulting from mass loss during the explosion. In addition, newly born compact objects receive natal kicks which are given by a Maxwellian distribution with a 1D rms of $\sigma = 265\,\mathrm{km\,s}^{-1}$, based on the observed distributions of radio pulsars (Hobbs et al. 2005). The kicks are lowered proportional to the amount of fall back as described in Section 4.5 of Fryer et al. (2012). An exception is made for neutron stars formed through electron capture supernovae for which no natal kicks are assumed in this simulation. As a result of this the mergers of double neutron stars are biased toward neutron stars formed through electron capture supernovae.

Submodel A and B— To consider the large uncertainties concerning binaries that begin Roche-lobe overflow while the donor star crosses the Hertzsprung gap, we consider two extreme cases. In submodel A we consider all common envelope formation channels including donor stars in any post main sequence evolutionary stage. In submodel B we explicitly exclude all evolutionary channels where the common envelope is initiated by a Hertzsprung gap donor star. Submodel B can be considered as a more conservative estimate of the merger rates for NS-NS, BH-NS, and BH-BH binaries (Belczynski et al. 2007). A detailed study and revision of criteria for the onset of common envelope will be presented shortly (Belczynski, Pavlovskii & Ivanova, in prep.).

Metallicity— With the reach of advanced LIGO/Virgo mergers will originate from all sorts of environments with high and low metallicity. We therefore consider two representative metallicities $Z = 0.02$ (typical of solar neighborhood) and $Z = 0.002$ (typical of small starburst galaxies). The physically consistent way to derive merger rates would be to start from an appropriate star formation history in the Universe, adopt a model of metallicity evolution with redshift and then calculate broad range of population synthesis models with varying metallicity in order to obtain current rate of mergers (O'Shaughnessy et al. 2008, 2010; Dominik et al. 2013, 2015). Given the scope of this study we adopt a simpler approach and take an even mix of these two compositions as a crude representation of metallicity distribution in local Universe (e.g. Panter et al. 2008). Although simplified, this is sufficient to judge the overall impact of the change in initial conditions and their associated uncertainties.

Difference with respect to Dominik et al. (2012) — Since the publication of the population synthesis calculations by Dominik et al. (2012), it was found that a technical bug was introduced during one of the annual code updates, related to the treatment of tidal locking. For detached binaries, in which both stars reside well within their Roche lobe, the effect of tides on the stellar and orbital spin is negligible. In such systems, the spins of the stars are typically not synchronized with the orbital motion. As the stars evolve they change their spin period, for example as a result of evolutionary expansion. At some point the spin and orbital period may become comparable. Such a system appears to be synchronized, at least momentarily, even though tides are not effective. The simulations by Dominik et al. (2012) incorrectly treated these systems as tidally locked, resulting in an incorrect further orbital evolution for specific cases. In general, this resulted in shrinking of the binary system with the overall effect of over predicting the double compact object merger rates.

For majority of the cases the differences are small: within factor of ~ 2, i.e. comparable to differences arising from the change of initial conditions. This can be seen when comparing the results before the correction given in Table 2 and 3 of Dominik et al. (2012), the standard model marked "S" in their paper and our results for the same assumptions, but after correction for the bug, as we provide in our Table 1, marked as the old standard model, "O".

In two cases, both for solar metallicity submodels B, involving binary merges with black holes the differences are larger. The BH-NS Galactic merger rate was revised from 0.2 Myr^{-1}(Dominik et al. 2012) to 0.06 Myr^{-1}(current study). The BH-BH Galactic merger rate was revised from 1.9 Myr^{-1}(Dominik et al. 2012) to 0.22 Myr^{-1}(current study).

Although the changes for these high metallicity channels are substantial, we repeat that the overall rate is completely dominated by the low metallicity channels. Therefore the impact of this correction on the overall compact merger rates, masses and delay times presented by (Dominik et al. 2012, 2013, 2015) is negligible.

3.2. Computation of the merger rates

We randomly draw binary systems from the initial distribution functions, once for high metallicity ($Z = 0.02$) and once for low metallicity ($Z = 0.002$). For computational efficiency we only select binary systems that are massive enough, within some safety margin, to potentially produce a double compact object involving a neutron star or a black hole. For primaries we take $M_1 \geq 5\ M_\odot$ and for secondaries $M_2 \geq 3\ M_\odot$.

Using the StarTrack population synthesis code we evolve $N_{\mathrm{sim}} = 2 \times 10^6$ of such binary systems. We estimate the mass formed in our simulations. To obtain the total mass in stars down to the lower stellar mass limits we integrate over the full extent of the initial mass function ($0.08 - 150\mathrm{M}_\odot$) and mass ratio distribution. We include the appropriate mass for single stars when needed. For this we assume that for each binary system with a primary mass M_1, there are $(1 - f_{\mathrm{bin}})/f_{\mathrm{bin}}$ single stars with a mass $M = M_1$

We present our rates in terms of the rate for a fiducial Galaxy, $\mathcal{R}_{\mathrm{gal}}$. We chose to adopt the exact same method as Dominik et al. (2012) to allow for comparison. We therefore assume a 10Gyr continuous star formation rate $\eta_{\mathrm{SFR}} = 3.5\ M_\odot\ \mathrm{Myr}^{-1}$. The resulting total mass formed in stars is within a factor of two of the estimates for the present-day stellar mass in the Milky Way[2]. The star formation history of our galaxy is not well known (e.g. Wyse 2009) but there is evidence for several discrete epochs of enhanced of star formation (e.g. Cignoni et al. 2006). The assumption of continuous star formation may be a rather crude approximation for the Milky Way itself. It may however serve as the rate for a fiducial Milky Way-like galaxy obtained after averaging over the LIGO detection volume.

In Table 1 we provide the rates for the different simulations. These rates can be converted into approximate volumetric rates, as used by the LIGO/Virgo collabora-

tion, with the following expression.

$$\mathcal{R}_{\mathrm{vol}} = 10\ \mathrm{yr}^{-1}\ \mathrm{Gpc}^{-3}\ \left[\frac{\rho}{0.01\mathrm{Mpc}^{-3}}\right]\left[\frac{\mathcal{R}_{\mathrm{gal}}}{\mathrm{Myr}^{-1}}\right] \quad (9)$$

where ρ is the local density of Milky Way like galaxies and R_{gal} the Galactic merger rate.

The detailed choices on how to normalize the rates are, to some extent, arbitrary. This is a result of the uncertainties in the low mass binary fraction and the poorly constrained distribution of their mass ratios. We chose to adopt very simple assumptions and we assume for the sake of this study that both binary fraction and mass ratio distribution adopted in a given model for massive stars hold true for the entire considered mass range ($0.08 - 150\mathrm{M}_\odot$).

Our Monte Carlo simulations are subject to statistical fluctuations due to they finite size. We estimate this by counting the total number of double compact objects that merge with 10 Gyr in each simulation, N_{x}, considering NS-NS, BH-NS, BH-BH separately. We use $1/\sqrt{N_x}$ as an approximation for the statistical uncertainty.

4. RESULTS: DISTRIBUTIONS

4.1. Comparison of the initial distributions

The effective initial distributions for all systems with a primary mass of at least $7\ M_\odot$ are shown in Fig. 1 for the old and new assumptions. Systems with lower primary masses are not capable of producing double neutron stars in our simulations. The histograms are shown for a metallicity $Z = 0.02$ and normalized to unity. The main differences between the old and new assumption concern (a) the period/separation distribution and (b) the eccentricity distribution.

Periods and separations — The main difference between old and new assumptions concerns the tightest systems. The new distributions show a clear preference for short periods / small separations as can be seen in central top and bottom panels of Fig. 1. The old distribution is flat for large separations but tight systems ($a \lesssim 100\ R_\odot$) are strongly suppressed. This is a result of the adopted lower limit a_{min}, which depends on the eccentricity and the stellar radii (see Sect. 2). Such a turnover is not observed for massive binaries. Even though we do not know at present how such close systems form, they exist and must be accounted for in the simulations as we do in the new initial conditions.

Eccentricities — The second main difference concerns the eccentricities (depicted in the top right panel of Fig. 1). The distribution adopted in the old simulations is the thermal distribution which strongly favors eccentric systems. The new distribution favors (near) circular systems. The high eccentricities in the old simulations allow much wider systems to still interact as discussed below.

Periastron separations — The distribution of periastron separations $d_{\mathrm{per}} = a(1 - e)$, i.e. the distance of closest approach at zero age, is shown in the bottom right panel in Fig. 1. To first order this is the most relevant parameter governing when systems start to interact by tides and later mass transfer. The old simulations favor wider and more eccentric systems, while the new simulations favor

---

[2] Estimates for the total stellar mass by Flynn et al. (2006) yields $4.85 - 5.5 \times 10^{10}\ M_\odot$ and $6.43 \pm 0.63 \times 10^{10}\ M_\odot$ by McMillan (2011).
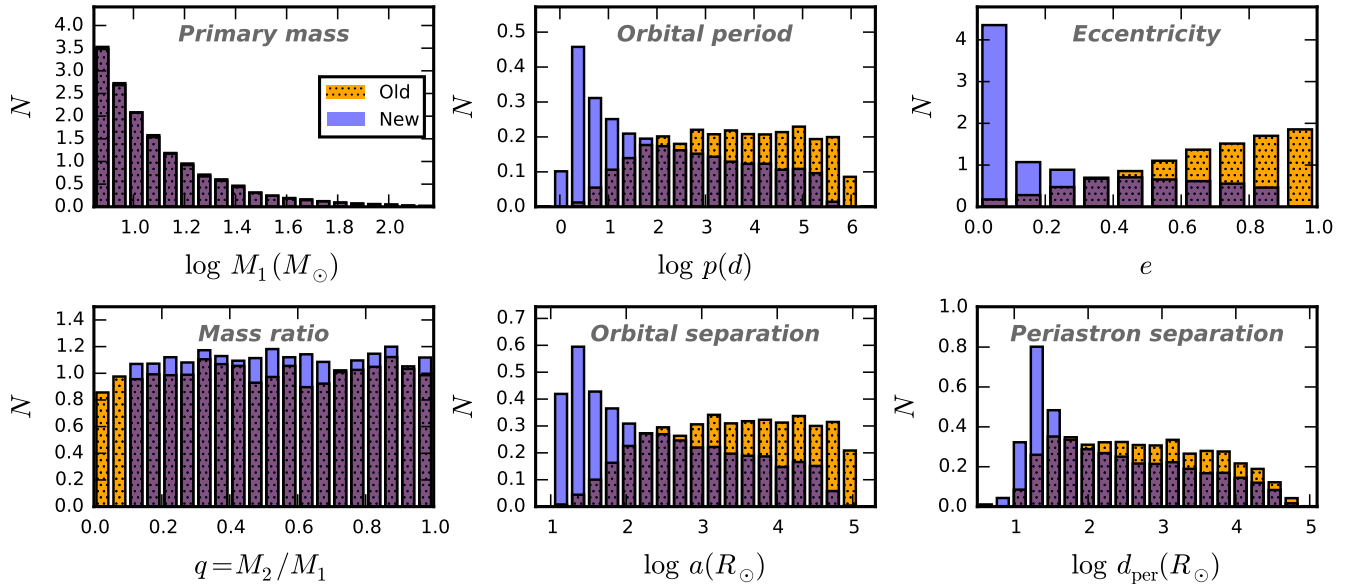
Fig. 1.— Distributions of initial parameters for the simulated systems resulting from the old and new assumptions. All histograms are normalized to unity.

tighter and more circular systems. By coincidence, these changes partially compensate each other.

The old assumptions resulted in a nearly flat distribution of periastron separations extending from $\log d_{per}(R_\odot) = 1\text{-}5$, being nearly flat between $\log d_{per}(R_\odot) = 1.5\text{-}4$ and turning over on both ends. Instead the new distributions peak at short periastron separations of about $10\text{-}50 R_\odot$ and gradually decay for higher separations.

However, in the regime of relevance for the formation of double compact objects ($\log d_{per}(R_\odot) = 1.5\text{-}4$, as we will see in the next section) both, old and new, periastron distribution are rather similar. We note only a slight domination of old distribution in this regime. The distributions in this figure are normalized to unity. The larger overall binary fraction in the new simulations will compensate for this.

Primary masses and mass ratios— In both simulations the mass ratios are drawn from a flat seed distribution (the bottom left panel of Fig. 1). They only differ in the adopted boundaries. In the old simulation companion masses are drawn down to the hydrogen burning limit. In the new simulations the minimum mass ratio adopted is $q_{min} = 0.1$. In our simulations with old initial distributions we found no double compact objects resulting from systems with such extreme mass ratio. This difference therefore only has a very minor effect on the final normalization.

The distributions of initial primary masses M_1 (shown in the top left panel of Fig. 1) are identical in both simulations. The only differences are stochastical in nature.

4.2. *Comparison of the birth properties of the progenitors of double compact object mergers*

Only a very small subset of the simulated binaries produces two compact objects that are bound and that will merge within 10 Gyr. The birth properties of this subset are shown in Fig. 2, where we compare the impact of the old and new assumptions for the initial conditions.

Note that the histograms are normalized to unity to allow comparison of the shape of the distribution, the resulting rates are discussed below. We separately show results for low metallicity (Z = 0.002, top panels) and high metallicity (Z = 0.02, bottom panels).

Since the trends observed when comparing the old and new initial distributions are very similar for submodel A and B, we chose to only show the results submodel B here. This is the more conservative submodel which excludes progenitor systems in which a Hertzsprung gap star acts as donor star during CE phase, see Section 3.1. In practice this means that on average the progenitors in model B result from wider systems and show a slightly stronger preference for equal mass progenitor systems. Data for submodel A (as well as data subdivided by the double compact object type) can be obtained from the online data repository for readers that are interested. More insight in the differences between submodel A and B can be found in (Dominik et al. 2012).

Primary masses— The distribution of initial primary masses of the progenitors consists of separate components. The narrow low mass peak around $10 M_\odot$ is generated by the progenitors of double neutron stars. The high mass component is only prominent in the low metallicity simulations. This component consists of the progenitors of mergers that involve a black hole.

The minimum initial mass to form a black hole is $40 M_\odot$ for the primary star of a double compact object progenitor at $Z = 0.02$. This is much higher than the minimum mass for a single star (or star in a very wide non interacting binary) to form a black hole in our simulations, which is $21 M_\odot$ at $Z = 0.02$. The difference is the result of the additional mass loss experienced in binary systems due to Roche lobe overflow and common envelope ejection from BH progenitor. At lower metallicity these minimum masses decrease. At $Z = 0.002$ we find a minimum initial mass of about $20 M_\odot$ for the primary star
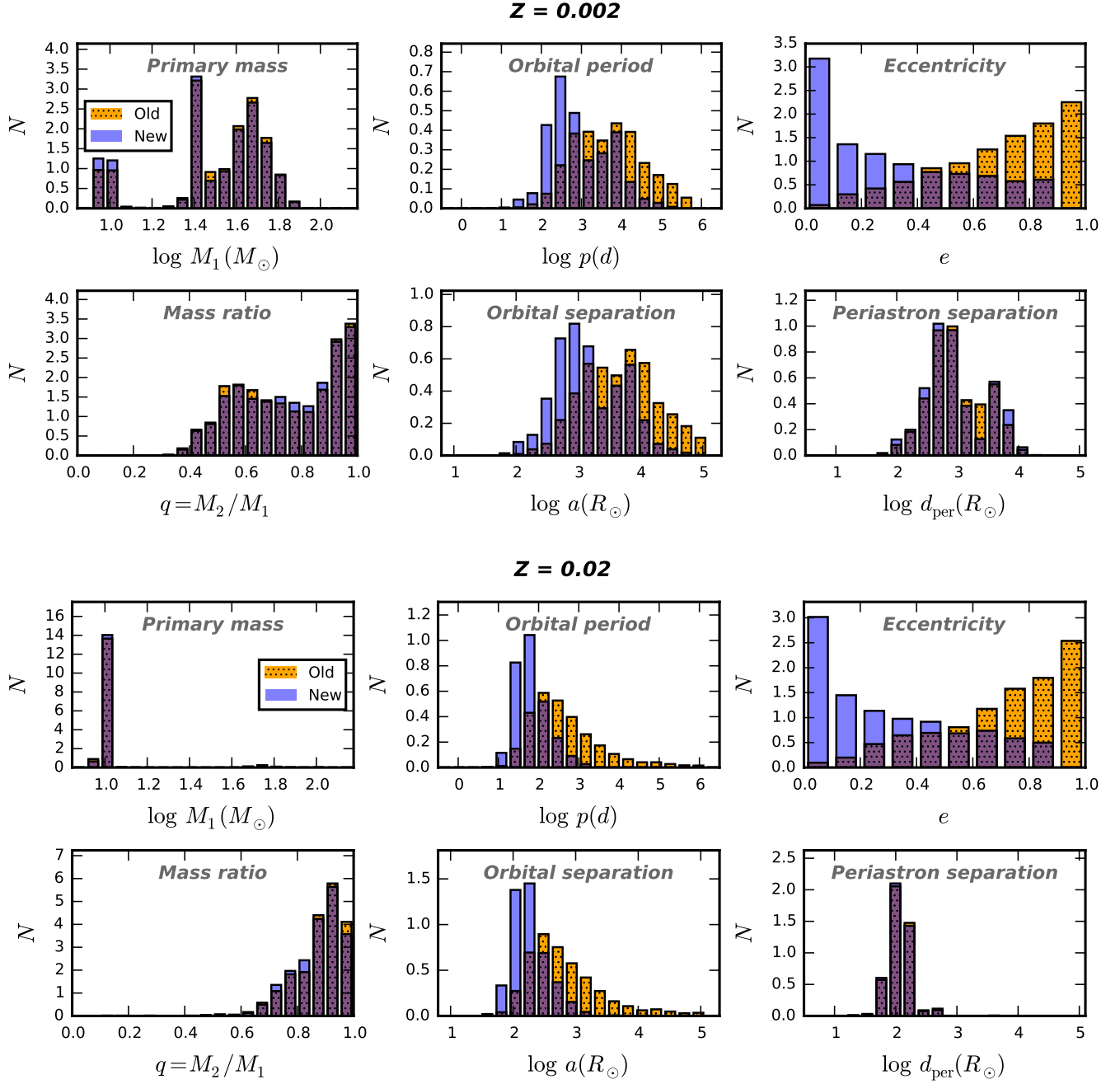
FIG. 2.— Birth distributions of initial binary parameters for the progenitors of double compact object mergers. The normalized histograms show the distributions for submodel B combining all types of mergers, for low and high metallicity.

of a double compact object progenitor involving a black hole.

The difference between the old and new simulations is very small. At low metallicity there is a slight tendency towards lower mass progenitors (favoring NS-NS progenitors) in the new simulations.

Mass ratios— For both the old and new simulations we find that the progenitors exclusively result from systems with mass ratios larger than about $M_2/M_1 \gtrsim 0.4$ at low metallicity and about 0.6 at high metallicity. For both metallicities there is a preference for progenitors with very equal masses, i.e. 0.9 and higher.

The difference between the old and new simulations is marginal, unsurprisingly given the similarity of the input distribution. A very slight tendency for the old simulations to favor more equal mass systems is observed at high metallicity, while the opposite behavior is observed at low metallicity. However, the differences are insignificant in comparison with the model uncertainties.

Periods, separations and eccentricities— The initial period and separation distributions of the progenitor systems show a clear difference between the old and new initial conditions. For both metallicities the old simulations are biased towards wider systems than the new
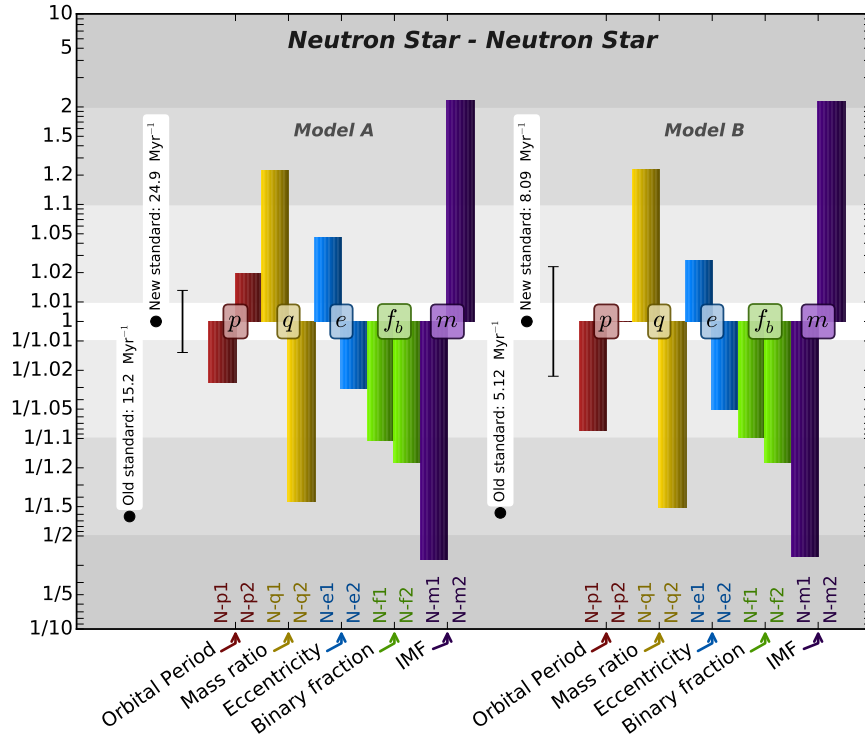
Fig. 3.— Variations in the merger rate predictions double neutron stars for the old and new standard assumptions and the effect of the allowed variations in the initial distributions of binary parameters. See also Table 2. Note that the Poisson variations (indicated as error bars) resulting from the finite size the number of simulated systems are comparable with some of the variations. We use a double mirrored logarithmic vertical axis to visualize the very small variations we obtain in most cases. For comparison, uncertainties from other sources (e.g., evolutionary uncertainties) are typically an order of magnitude or more.

simulations. At high metallicity the distributions peak near $150R_\odot$ in the new simulations and near $300R_\odot$ in the old simulations. At low metallicity the distribution is clearly bimodal peaking around 800 and $8000R_\odot$ in the new simulations.

The distribution of initial eccentricities of merger progenitors closely reflects the shape of the input distribution of the population, although in both cases systems with larger eccentricities are over represented.

Periastron separations — Although the distributions of initial separations a and eccentricities e are very different between the old and new simulations, the distribution of initial periastron separations d_{per} of merger progenitors is nearly indistinguishable.

For low metallicity the distribution is again bimodal. Detailed inspection of the evolutionary paths of the systems that populate both peaks show that the tighter systems first evolve through a stable mass transfer phase. The wider systems first evolve through a common envelope phase. These evolutionary channels are identified and described in earlier work (Dominik et al. (2012); see their Table 5 and associated text).

Both channels exist in the old and new simulations, since the input physics assumptions are not changed. The similarity in the periastron separation distributions implies that the relative contribution of both channels did not significantly change when switching from the old to new assumptions.

4.3. *Distributions of final properties*

The distribution of the final properties predicted by our simulations that are of interest for gravitational wave searches include the delay times, component masses, mass ratios and chirp masses. Detailed models of the anticipated waveforms will enable the inference on several parameters, such as component masses (Aasi et al. 2013a; Veitch et al. 2015) and if multiple events are detected constraints on the properties of the population can be inferred (Mandel 2010; Mandel et al. 2015).

We find that the distributions of final properties are remarkably insensitive to the assumed initial conditions. The predicted distribution of the component masses, mass ratios, chirp masses and delay times show no significant changes when the initial conditions are varied within current uncertainties. They are almost identical to those presented by Dominik et al. (2012), to which we refer for detailed discussion.

The insensitivity of rate predictions results from the (coincidental) similarity of the initial periastron separation distribution and the mass ratio distribution, which remained practically unchanged. These two parameters are key in determining the fate of the binary system (and thus merger rates). However, the physical properties of merging binaries are not sensitive to changes in initial conditions.

There are relatively few formation channels for double compact object mergers. For a given model of evolution, these formation channels originate from a rather narrow volume of initial parameter space ("the formation volume"). Change of initial conditions alters the number of the progenitor binaries in the formation volume, but has
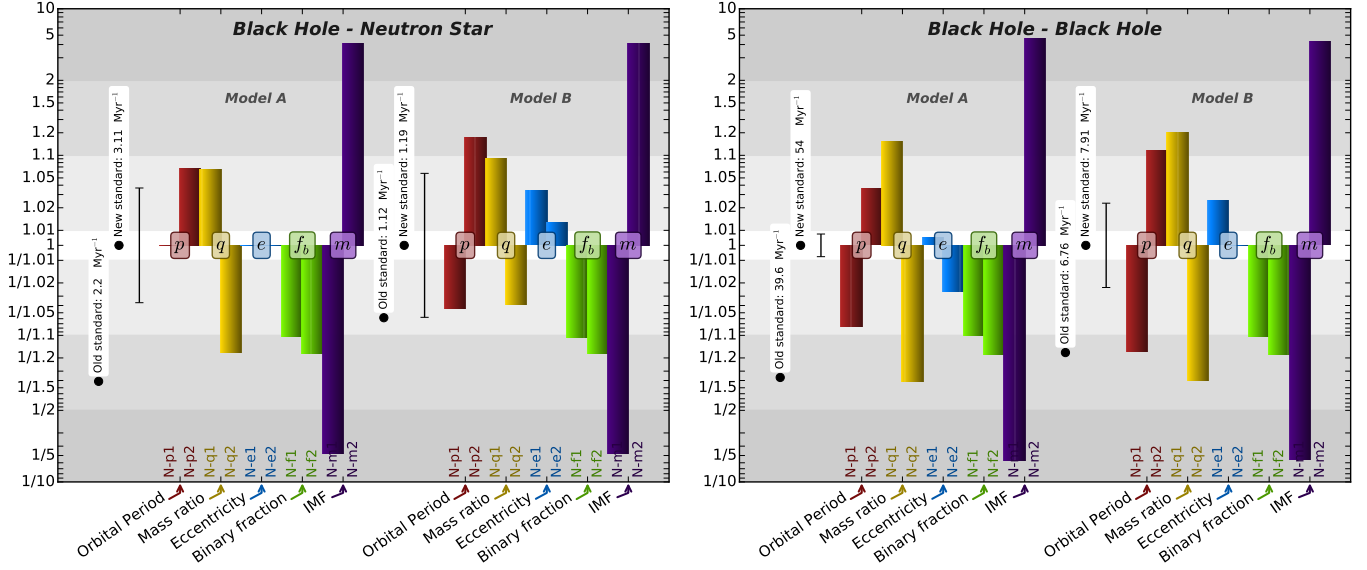
FIG. 4.— As Fig. 3 for the merger rates BH-NS (left) and BH-BH (right) systems.

very little effect on the binary merger properties. This insensitivity is not just connected to the specific initial conditions considered here, but is of more fundamental nature. It is a robust result that has also been found in connection to other compact object binaries. For example by Kalogera & Webbink (1998) in the context of low-mass X-ray binaries, and see also Belczynski et al. (2002).

The robustness of the final distributions against initial condition uncertainties considered here, but also wider variations, is reassuring in the light of anticipated gravitational wave detections. It removes one layer of uncertainties and allows for more optimism concerning the potential of such detections for constraining more interesting aspects such as the physics uncertainties.

The final properties of our simulations are available through our online data files available at (www.syntheticuniverse.org).

5. RESULTS: MERGER RATES

In Table 1 we list the double compact object merger rates for our new standard model N, the old standard model O, and variations on the models that explore the effect of uncertainties in initial distributions. All rates are expressed as the rate for a fiducial Milky Way Galaxy as detailed in Sect 3.2. We give the results both for submodel A and the more conservative submodel B. Merger rates are also presented separately for low ($Z = 0.002$) and high metallicity ($Z = 0.02$) stellar and binary evolution.

In Table 2 we present merger rates that correspond to a fiducial Galaxy with an even mix (50%–50%) of low-metallicity ($Z = 0.002$) and high-metallicity ($Z = 0.02$) stars. Absolute mixed merger rates are given only for our new standard model (an average of low- and high-metallicity fiducial Galactic rates from Table 1) and can be readily obtained for any other model. For all other models only relative change of rates with respect to our new standard is given. A graphical representation of the changes relative to the new standard model is given in Figure 3.

The overall conclusions are: (i) merger rates increase slightly with the new assumptions, and they are within a factor of 2 of old standard rates; (ii) merger rates change by less than factor of 2 within associated uncertainties embedded in new initial distributions concerning binary parameters (the only exception being the IMF). These conclusions hold for all types of double compact object mergers (NS-NS, BH-NS and BH-BH) and the changes are typically much smaller than the maxima listed above. In the following section we discuss the various trends.

5.1. Impact of the new initial conditions

The adoption of the new assumptions for the initial conditions leads to higher estimates for all merger rates. The largest change is found when adopting model A. The old rates are 39% lower than the new rates for NS-NS mergers, 29% lower for BH-NS mergers and 27% lower for BH-BH mergers. An overview of the relative changes is given in Tab. 2 using the new standard rate as reference.

When adopting submodel B the observed changes are even smaller in the case of BH-NS and BH-BH mergers. The submodel B excludes progenitor channels which involve common envelope evolution with a Hertzsprung gap donor (Belczynski et al. 2007). These typically come from progenitor binaries with smaller initial separations where the old and new distributions deviate most strongly. Excluding these progenitors reduces the difference between old and new simulations. For the BH-NS in submodel B the changes are so small that they are of the same order as the expected statistical fluctuations resulting from the finite number of systems in our simulations. These average statistical fluctuations are shown in Figure 3 as an errorbars.

The main reason for the slight increase in the merger rate is the large binary fraction adopted in the new initial conditions ($f_b = 1$). The old distributions with the high binary fraction of $f_b = 1$ (model O-f1) give merger rates that are higher (up to $\sim 50\%$ in the case of BH-NS mergers in submodel B) than for the new standard model (see Table 2).

5.2. *Variations due to uncertainties in the new initial conditions*

All relative merger rate changes are smaller than 34% for *all* types of double compact objects when varying the initial conditions concerning binary properties (models N-p1, N-p2, N-q1, N-q2, N-e1, N-e2, N-f1, N-f2; see Tab. 2). This is not true for variations in the IMF, which we will discuss at the end of this paragraph.

The initial distribution of mass ratios that rather steeply falls off with mass ratio (model N-q2) is the cause of merger rate decrease of the order of $\sim 30\%$ for NS-NS and BH-BH mergers. A distribution favoring equal mass systems at birth mildly favors the formation of NS-NS systems and BH-BH systems. The BH-NS mergers show the same trend, but the changes are comparable to the Poison fluctuations. Varying the initial period distribution has a smaller effect, below 20% and approaching our statistical uncertainties. A flatter period distributions, i.e. one that favors wider systems (model N-p2), results in a more effective formation of compact object mergers. A period distribution favoring short period systems more strongly (model N-p1) mainly adds systems that interact or merge prematurely, preventing the formation of a double compact object system. Varying the eccentricity distribution within the ranges given by Sana et al. (2012) has no significant effect on the merger rates. All variations found are less than 5% for all submodels and all types of mergers considered. These variations are dominated by the statistical fluctuations in our Monte Carlo simulations. A reduction of the total binary fraction to $f_{\rm bin} = 0.85$ (which roughly corresponds to the one sigma lower limit of intrinsic spectroscopic binary fraction, $f_{\rm sp} = 0.7 \pm 0.1$, derived by Sana et al. 2012) leads to a reduction of all compact object merger rates by 10% (model N-f1). A further reduction of the total binary fraction to $f_{\rm bin} = 0.7$ (model N-f2), which roughly corresponds two the two sigma lower limit on the observational constraints, reduces the merger rates by 15%.

Significant change of the power law exponent of the IMF for stars more massive than $1{\rm M}_\odot$ generates the largest change of double compact merger rates in our suite of models. We allow for a change of the exponent by 0.5 up and down from our standard value $\alpha = 2.7$. Note that this affects the mass distribution of the primary stars in binary systems and single stars for those models where $f_{\rm bin} < 1$ (model O-f1, N-f1, N-f2). Merger rates decrease within a factor of 2.7 for NS-NS mergers, a factor of 4.8 for BH-NS mergers and a factor of 5.8 for BH-BH mergers for our most steep IMF (model N-m1) in respect to our new standard model (N). Merger rates increase within a factor of 2.2 for NS-NS mergers, a factor of 4.1 for BH-NS mergers and a factor of 4.7 for BH-BH mergers for our most flat IMF (model N-m2). These changes are due to two effects. First, the steeper the IMF the fewer double compact objects form in a population of binary stars. The heaviest BH-BH mergers are affected the most. Second, the slope of high-mass IMF has a significant impact on the total mass of the fiducial Galaxy. For the same number of massive binary stars that we draw from initial distributions ($N_{\rm sim} = 2 \times 10^6$) the corresponding total mass of simulation (over the entire stellar mass range) is ~ 2.5 higher and ~ 2.5 smaller for our model with the steep and flat IMF, respectively as compared with our adopted standard IMF.

6. DISCUSSION AND CONCLUSION

Recently, Sana et al. (2012) have presented measurements of initial binary parameters for massive stars. These measurements, in some aspects, are in stark contrast with so far used assumptions in evolutionary studies of massive stars (e.g. Belczynski et al. 2002; Voss & Tauris 2003; Dominik et al. 2012; Mennekens & Vanbeveren 2014). The old standard prescriptions (a flat distribution in log separation, a thermal eccentricity distribution strongly favoring eccentric systems and typically an adopted binary fraction of 50% counting systems with separations up to $10^5\,R_\odot$) may still apply for low- and intermediate-mass stars, but the new measurements show very different initial binary parameter distributions for massive stars (strong overabundance of very tight systems, a binary fraction that reaches 100% when including systems up to about $10^{4.5}{\rm R}_\odot$ and mostly circular systems).

We find a small increase in the NS-NS, BH-NS and BH-BH merger rate as a result of the new initial conditions (due to the increased binary fraction), with the old rates being up to 40% lower than the new rates. Secondly, we study the impact of the allowed variations of the new binary parameter distributions within the observational uncertainties. We find that they have negligible impact (typical variations of a few percent, always less than a factor of 2). All changes are negligible in comparison with the evolutionary model uncertainties (which are typically 1-2 orders of magnitude; e.g., Dominik et al. 2012).

The only exception to our above conclusion are the variations of double compact merger rates due to the uncertainty in the slope of the IMF for stars more massive than $1{\rm M}_\odot$. These variations can be as high as factor of $\sim 3, 4, 6$ up and down for NS-NS, BH-NS and BH-BH mergers, respectively from our new reference model that employs the best estimates on the initial conditions for massive binaries. This is due to the change of the overall mass of the stellar mass content which is used to normalize the rates and to the diminishing number of double compact object progenitors with the increasing steepness of the IMF.

The small impact of the new distributions of binary properties on the merger rates is somewhat counter-intuitive. This result stems from the fact that major changes in the initial binary parameter distributions cancel out in the regime important for close double compact object formation. Although, new distributions show a much stronger bias toward close binary orbits in comparison to the old distributions, the periastron distance distribution is similar to the one generated by old distributions in the regime $1.5 < \log(d_{\rm per}/{\rm R}_\odot) < 4$ (see Fig. 1). This is because of the strong preference for very eccentric systems adopted in the older distributions, for which there is no supported in the new observations (mostly circular orbits). This regime of periastron separations plays a crucial role in the formation of stellar-mass double compact object mergers (see Fig. 2). The periastron distance is key in determining when tides become important and when the primary star fills its Roche lobe for the first time. Since the distribution of component masses is very similar, it is the periastron separation that largely

TABLE 1
MERGER RATES FOR A FIDUCIAL MILKY WAY GALAXY [MYR^{-1}]

Model ID	NS-NS A	NS-NS B	BH-NS A	BH-NS B	BH-BH A	BH-BH B	NS-NS A	NS-NS B	BH-NS A	BH-NS B	BH-BH A	BH-BH B	Description
	Z = 0.002						**Z = 0.02**						
N	12.8	3.68	4.45	2.32	98.3	15.6	36.9	12.5	1.77	0.06	9.73	0.22	new standard
O	8.17	2.43	3.17	2.24	72.2	13.3	22.3	7.82	1.24	0.01	6.98	0.22	old standard
O-f1	13.2	3.92	5.11	3.60	116	21.5	35.9	12.6	1.99	0.02	11.3	0.36	old, $f_{\rm bin} = 1.0$
N-p1	12.5	3.34	4.72	2.23	90.8	13.3	35.9	11.6	1.46	0.05	9.46	0.29	new, $(\log p)^{-0.75}$
N-p2	13.4	3.67	4.64	2.75	102	17.5	37.3	12.6	2.00	0.05	9.87	0.20	new, $(\log p)^{-0.35}$
N-q1	16.3	4.28	5.15	2.53	113	18.8	44.7	15.6	1.48	0.07	11.7	0.24	new, $q^{0.5}$
N-q2	8.65	2.52	4.00	2.23	69.8	11.1	25.7	8.17	1.32	0.06	6.84	0.13	new, $q^{-0.7}$
N-e1	13.2	3.71	4.49	2.40	99.0	16.0	38.8	12.9	1.70	0.06	9.93	0.22	new, $e^{-0.59}$
N-e2	12.7	3.41	4.66	2.37	95.3	15.7	35.5	12.0	1.57	0.04	9.90	0.12	new, $e^{-0.25}$
N-f1	11.6	3.34	4.03	2.09	89.1	14.1	33.4	11.4	1.60	0.06	8.84	0.20	new, $f_{\rm bin} = 0.85$
N-f2	10.9	3.13	3.78	1.97	83.4	13.2	31.3	10.6	1.51	0.05	8.26	0.19	new, $f_{\rm bin} = 0.7$
N-m1	4.70	1.43	0.99	0.49	17.2	2.77	13.4	4.65	0.31	0.01	1.54	0.04	new, $m_1^{-3.2}$
N-m2	26.5	7.80	17.9	9.51	457	66.9	81.3	26.9	7.86	0.32	51.4	1.19	new, $m_1^{-2.2}$

NOTE. — [a]Rates correspond to a galaxy with 10 Gyr of constant star formation rate at the level of $3.5 M_\odot$ yr^{-1} as detailed in Section 3.2. Rates are given for low and high metallicity and for two different model assumptions. In model A we allow for high rate of common envelope survival, while more the conservative model B does not allow the formation of double compact objects for donors on Hertzsprung gap.

TABLE 2
RELATIVE CHANGES OF MIXED-METALLICITY MERGER RATES[a]

Model ID	NS-NS A	NS-NS B	BH-NS A	BH-NS B	BH-BH A	BH-BH B	Description
N	1.000	1.000	1.000	1.000	1.000	1.000	new standard
	(24.85)	**(8.090)**	**(3.110)**	**(1.190)**	**(54.02)**	**(7.910)**	absolute rates [Myr^{-1}]
O	0.613	0.633	0.709	0.945	0.733	0.855	old standard
O-f1	0.988	1.021	1.141	1.521	1.178	1.382	old, $f_{\rm bin} = 1.0$
N-p1	0.974	0.923	0.994	0.958	0.928	0.859	new, $(\log p)^{-0.75}$
N-p2	1.020	1.006	1.068	1.176	1.036	1.119	new, $(\log p)^{-0.35}$
N-q1	1.227	1.229	1.066	1.092	1.154	1.204	new, $q^{0.5}$
N-q2	0.691	0.661	0.855	0.962	0.709	0.710	new, $q^{-0.7}$
N-e1	1.046	1.027	0.995	1.034	1.008	1.025	new, $e^{-0.59}$
N-e2	0.970	0.952	1.002	1.013	0.974	1.000	new, $e^{-0.25}$
N-f1	0.905	0.911	0.905	0.903	0.907	0.904	new, $f_{\rm bin} = 0.85$
N-f2	0.849	0.849	0.850	0.849	0.848	0.846	new, $f_{\rm bin} = 0.7$
N-m1	0.364	0.376	0.209	0.210	0.173	0.178	new, $m_1^{-3.2}$
N-m2	2.169	2.145	4.141	4.130	4.706	4.304	new, $m_1^{-2.2}$

NOTE. — Rates correspond to a fiducial Milky Way Galaxy with an even mix (50%–50%) of low-metallicity ($Z = 0.002$) and high-metallicity ($Z = 0.02$) stars (the average of low- and high-metallicity fiducial Galactic rates from Table 1). We give all rates relative to our new standard model. A graphical representation is shown in Figure 3.

determines the future evolution of the binary system. It happens (by pure coincidence) that the old prescriptions and the new measurements result in rather similar orbital separations at the time of the first mass transfer for progenitors of double compact objects. Additionally, the observational uncertainties of the new estimates of initial binary parameters for massive stars are not large enough to cause significant NS-NS, BH-NS and BH-BH merger rate changes. Similarly, we find that the distributions of final properties (delay-times and final component masses) are insensitive to the variations of initial conditions. The summary of our merger rate analysis is given in Fig. 3.

Our study allows to eliminate one layer of uncertainties involved in population synthesis predictions for double compact object mergers. Such predictions are infamous for their number of poorly constrained model parameters. Recent years of intensive studies of double compact object formation have proven that it is extremely hard (yet, not impossible) to identify a well posed non-degenerate problem with population synthesis. This fact does not reflect the intrinsic weakness of the population synthesis method, but rather the lack of understanding of some basic processes involved in the evolution of massive single (e.g., convection, rotation, supernova/core collapse) and binary stars (e.g., tidal interactions, common envelope evolution).

The reduction of the modeling uncertainties, like the one presented here, is crucial for advancement of our understanding of the remaining poorly constrained physi-

cal processes involved in double compact object formation. The further reduction of the uncertainties may potentially allow gravitational-wave observatories to assess and constrain physical processes that are thus far beyond the reach of electromagnetic observations and theoretical studies.

REFERENCES

Aarseth, S. J. 2012, MNRAS, 422, 841
Aasi, J., et al. 2013a, Phys. Rev. D, 88, 062001
—. 2013b, ArXiv e-prints 1304.0670
—. 2013c, Phys. Rev. D, 87, 022002
Abadie, J., et al. 2010, Classical and Quantum Gravity, 27, 173001
—. 2012, Phys. Rev. D, 85, 082002
Abate, C., Pols, O. R., Izzard, R. G., Mohamed, S. S., & de Mink, S. E. 2013, A&A, 552, A26
Abbott, B. P., et al. 2009, Reports on Progress in Physics, 72, 076901
Abt, H. A. 1983, ARA&A, 21, 343
Banerjee, S., Baumgardt, H., & Kroupa, P. 2010, MNRAS, 402, 371
Bastian, N., Covey, K. R., & Meyer, M. R. 2010, ARA&A, 48, 339
Belczynski, K., Bulik, T., Fryer, C. L., Ruiter, A., Valsecchi, F., Vink, J. S., & Hurley, J. R. 2010, ApJ, 714, 1217
Belczynski, K., Dominik, M., Repetto, S., Holz, D. E., & Fryer, C. L. 2012a, ArXiv e-prints
Belczynski, K., Kalogera, V., & Bulik, T. 2002, ApJ, 572, 407
Belczynski, K., Kalogera, V., Rasio, F. A., Taam, R. E., Zezas, A., Bulik, T., Maccarone, T. J., & Ivanova, N. 2008, ApJS, 174, 223
Belczynski, K., Taam, R. E., Kalogera, V., Rasio, F. A., & Bulik, T. 2007, ApJ, 662, 504
Belczynski, K., Wiktorowicz, G., Fryer, C. L., Holz, D. E., & Kalogera, V. 2012b, ApJ, 757, 91
Bethe, H. A., & Brown, G. E. 1998, ApJ, 506, 780
Blaauw, A. 1961, Bull. Astron. Inst. Netherlands, 15, 265
Bloom, J. S., Sigurdsson, S., & Pols, O. R. 1999, MNRAS, 305, 763
Boersma, J. 1961, Bull. Astron. Inst. Netherlands, 15, 291
Brott, I., et al. 2011a, A&A, 530, A115
—. 2011b, A&A, 530, A116
Bulik, T., Belczynski, K., & Prestwich, A. 2011, ApJ, 730, 140
Burgay, M., et al. 2003, Nature, 426, 531
Cantrell, A. G., & Dougan, T. J. 2014, MNRAS, 445, 2028
Caron, B., et al. 1997, Classical and Quantum Gravity, 14, 1461
Chini, R., Hoffmeister, V. H., Nasseri, A., Stahl, O., & Zinnecker, H. 2012, MNRAS, 424, 1925
Cignoni, M., Degl'Innocenti, S., Prada Moroni, P. G., & Shore, S. N. 2006, A&A, 459, 783

Claeys, J. S. W., Pols, O. R., Izzard, R. G., Vink, J., & Verbunt, F. W. M. 2014, A&A, 563, A83
Clausen, D., Sigurdsson, S., & Chernoff, D. F. 2013, MNRAS, 428, 3618
De Donder, E., & Vanbeveren, D. 1998, A&A, 333, 557
—. 2004, New Astronomy, 9, 1
de Mink, S. E., Cantiello, M., Langer, N., Pols, O. R., Brott, I., & Yoon, S.-C. 2009, A&A, 497, 243
de Mink, S. E., Langer, N., Izzard, R. G., Sana, H., & de Koter, A. 2013, ApJ, 764, 166
de Mink, S. E., Sana, H., Langer, N., Izzard, R. G., & Schneider, F. R. N. 2014, ApJ, 782, 7
Dewi, J. D. M., Podsiadlowski, P., & Sena, A. 2006, MNRAS, 368, 1742
Dewi, J. D. M., & Pols, O. R. 2003, MNRAS, 344, 629
Dominik, M., Belczynski, K., Fryer, C., Holz, D. E., Berti, E., Bulik, T., Mandel, I., & O'Shaughnessy, R. 2012, ApJ, 759, 52
—. 2013, ApJ, 779, 72
Dominik, M., et al. 2015, ApJ, 806, 263
Duchêne, G., & Kraus, A. 2013, ARA&A, 51, 269
Dunstall, P. R., et al. 2015, A&A, 580, A93
Einstein, A. 1918, Sitzungsberichte der Königlich Preußischen Akademie der Wissenschaften (Berlin), Seite 154-167., 154
Ekström, S., et al. 2012, A&A, 537, A146
Flynn, C., Holmberg, J., Portinari, L., Fuchs, B., & Jahreiß, H. 2006, MNRAS, 372, 1149
Fong, W., et al. 2012, ApJ, 756, 189
Fragos, T., et al. 2013, ApJ, 764, 41
Fryer, C. L., Belczynski, K., Wiktorowicz, G., Dominik, M., Kalogera, V., & Holz, D. E. 2012, ApJ, 749, 91
Grishchuk, L. P., Lipunov, V. M., Postnov, K. A., Prokhorov, M. E., & Sathyaprakash, B. S. 2001, Physics Uspekhi, 44, 1
Grudzinska, M., et al. 2015, MNRAS, 452, 2773
Hamann, W.-R., & Koesterke, L. 1998, A&A, 335, 1003
Heggie, D. C. 1975, MNRAS, 173, 729
Hobbs, G., Lorimer, D. R., Lyne, A. G., & Kramer, M. 2005, MNRAS, 360, 974
Hulse, R. A., & Taylor, J. H. 1975, ApJ, 195, L51
Hurley, J. R., Pols, O. R., & Tout, C. A. 2000, MNRAS, 315, 543
Hurley, J. R., Tout, C. A., & Pols, O. R. 2002, MNRAS, 329, 897
Ivanova, N., Heinke, C. O., Rasio, F. A., Belczynski, K., & Fregeau, J. M. 2008, MNRAS, 386, 553

Izzard, R. G., Dray, L. M., Karakas, A. I., Lugaro, M., & Tout, C. A. 2006, A&A, 460, 565
Izzard, R. G., Glebbeek, E., Stancliffe, R. J., & Pols, O. R. 2009, A&A, 508, 1359
Izzard, R. G., Ramirez-Ruiz, E., & Tout, C. A. 2004, MNRAS, 348, 1215
Kalogera, V., & Webbink, R. F. 1998, ApJ, 493, 351
Kalogera, V., et al. 2004, ApJ, 601, L179
Kim, C., Kalogera, V., & Lorimer, D. 2010, New Astronomy Reviews, 54, 148
Kiminki, D. C., & Kobulnicky, H. A. 2012, ApJ, 751, 4
Kobulnicky, H. A., & Fryer, C. L. 2007, ApJ, 670, 747
Kobulnicky, H. A., et al. 2014, ApJS, 213, 34
Kochanek, C. S., Adams, S. M., & Belczynski, K. 2014, MNRAS, 443, 1319
Köhler, K., et al. 2015, A&A, 573, A71
Kroupa, P. 2002, Science, 295, 82
Kroupa, P., Tout, C. A., & Gilmore, G. 1993, MNRAS, 262, 545
Kroupa, P., & Weidner, C. 2003, ApJ, 598, 1076
Lipunov, V. M., Postnov, K. A., & Prokhorov, M. E. 1997, MNRAS, 288, 245
Lucy, L. B. 2006, A&A, 457, 629
Lyne, A. G., et al. 2004, Science, 303, 1153
Mandel, I. 2010, Phys. Rev. D, 81, 084029
Mandel, I., Haster, C.-J., Dominik, M., & Belczynski, K. 2015, MNRAS, 450, L85
Mandel, I., & O'Shaughnessy, R. 2010, Classical and Quantum Gravity, 27, 114007
Mason, B. D., Hartkopf, W. I., Gies, D. R., Henry, T. J., & Helsel, J. W. 2009, AJ, 137, 3358
McMillan, P. J. 2011, MNRAS, 414, 2446
Mennekens, N., & Vanbeveren, D. 2014, A&A, 564, A134
Mennekens, N., Vanbeveren, D., De Greve, J. P., & De Donder, E. 2010, A&A, 515, A89
Moe, M., & Di Stefano, R. 2013, ApJ, 778, 95
—. 2015a, ApJ, 801, 113
—. 2015b, ArXiv e-prints
Nelemans, G., Yungelson, L. R., & Portegies Zwart, S. F. 2001, A&A, 375, 890
Nomoto, K. 1984, ApJ, 277, 791
Nutzman, P., Kalogera, V., Finn, L. S., Hendrickson, C., & Belczynski, K. 2004, ApJ, 612, 364
Öpik, E. 1924, Tartu Obs. Publ., 25, 6
Orosz, J. A., McClintock, J. E., Aufdenberg, J. P., Remillard, R. A., Reid, M. J., Narayan, R., & Gou, L. 2011, ApJ, 742, 84
O'Shaughnessy, R., Belczynski, K., & Kalogera, V. 2008, ApJ, 675, 566
O'Shaughnessy, R., Kalogera, V., & Belczynski, K. 2010, ApJ, 716, 615
Panter, B., Jimenez, R., Heavens, A. F., & Charlot, S. 2008, MNRAS, 391, 1117
Pfahl, E., Podsiadlowski, P., & Rappaport, S. 2005, ApJ, 628, 343
Phinney, E. S. 1991, ApJ, 380, L17
Pinsonneault, M. H., & Stanek, K. Z. 2006, ApJ, 639, L67
Podsiadlowski, P., Joss, P. C., & Hsu, J. J. L. 1992, ApJ, 391, 246

Podsiadlowski, P., Langer, N., Poelarends, A. J. T., Rappaport, S., Heger, A., & Pfahl, E. 2004, ApJ, 612, 1044
Pols, O. R., Schröder, K.-P., Hurley, J. R., Tout, C. A., & Eggleton, P. P. 1998, MNRAS, 298, 525
Pols, O. R., Tout, C. A., Schröder, K.-P., Eggleton, P. P., & Manners, J. 1997, MNRAS, 289, 869
Postnov, K. A., & Yungelson, L. R. 2006, Living Reviews in Relativity, 9, 6
Prestwich, A. H., et al. 2007, ApJ, 669, L21
Ramirez-Ruiz, E., Trenti, M., MacLeod, M., Roberts, L. F., Lee, W. H., & Saladino-Rosas, M. I. 2015, ApJ, 802, L22
Ribas, I., Jordi, C., & Giménez, Á. 2000, MNRAS, 318, L55
Ruiter, A. J., Belczynski, K., & Fryer, C. 2009, ApJ, 699, 2026
Ruiter, A. J., Belczynski, K., Sim, S. A., Seitenzahl, I. R., & Kwiatkowski, D. 2014, MNRAS, 440, L101
Samsing, J., MacLeod, M., & Ramirez-Ruiz, E. 2014, ApJ, 784, 71
Sana, H., et al. 2012, Science, 337, 444
Sana, H., et al. 2013, A&A, 550, A107
—. 2014, ApJS, 215, 15
Schneider, F. R. N., Izzard, R. G., Langer, N., & de Mink, S. E. 2015, ApJ, 805, 20
Schneider, F. R. N., et al. 2014, ApJ, 780, 117
Silverman, J. M., & Filippenko, A. V. 2008, ApJ, 678, L17
Smith, N. 2014, ARA&A, 52, 487
Stevenson, S., Ohme, F., & Fairhurst, S. 2015, ArXiv e-prints 1504.07802
Szécsi, D., Langer, N., Yoon, S.-C., Sanyal, D., de Mink, S., Evans, C. J., & Dermine, T. 2015, A&A, 581, A15
Taylor, J. H., & Weisberg, J. M. 1989, ApJ, 345, 434
Toonen, S., Claeys, J. S. W., Mennekens, N., & Ruiter, A. J. 2014, A&A, 562, A14
Tout, C. A., Aarseth, S. J., Pols, O. R., & Eggleton, P. P. 1997, MNRAS, 291, 732
Vanbeveren, D., Mennekens, N., Van Rensbergen, W., & De Loore, C. 2013, A&A, 552, A105
Veitch, J., et al. 2015, Phys. Rev. D, 91, 042003
Vink, J. S., & de Koter, A. 2005, A&A, 442, 587
Vink, J. S., de Koter, A., & Lamers, H. J. G. L. M. 2001, A&A, 369, 574
Voss, R., & Tauris, T. M. 2003, MNRAS, 342, 1169
Webbink, R. F. 1984, ApJ, 277, 355
Wright, N. J., Drew, J. E., & Mohr-Smith, M. 2015, ArXiv e-prints
Wyse, R. F. G. 2009, in IAU Symposium, Vol. 258, IAU Symposium, ed. E. E. Mamajek, D. R. Soderblom, & R. F. G. Wyse, 11–22
Xu, X.-J., & Li, X.-D. 2010a, ApJ, 722, 1985
—. 2010b, ApJ, 716, 114
Yoon, S.-C., & Langer, N. 2005, A&A, 443, 643
Yungelson, L. R., Lasota, J.-P., Nelemans, G., Dubus, G., van den Heuvel, E. P. J., Dewi, J., & Portegies Zwart, S. 2006, A&A, 454, 559
Yusof, N., et al. 2013, MNRAS, 433, 1114
Zahn, J.-P. 1975, A&A, 41, 329